



A Journal of the Gesellschaft Deutscher Chemiker

Angewandte Chemie

GDCh

International Edition

www.angewandte.org

Accepted Article

Title: Solvent-Vapor-Induced Reversible Single-Crystal-to-Single-Crystal Transformation of a Triphosphaazatriangulene-based Metal–Organic Framework

Authors: Soichiro Nakatsuka, Yusuke Watanabe, Yoshinobu Kamakura, Satoshi Horike, Daisuke Tanaka, and Takuji Hatakeyama

This manuscript has been accepted after peer review and appears as an Accepted Article online prior to editing, proofing, and formal publication of the final Version of Record (VoR). This work is currently citable by using the Digital Object Identifier (DOI) given below. The VoR will be published online in Early View as soon as possible and may be different to this Accepted Article as a result of editing. Readers should obtain the VoR from the journal website shown below when it is published to ensure accuracy of information. The authors are responsible for the content of this Accepted Article.

To be cited as: *Angew. Chem. Int. Ed.* 10.1002/anie.201912195
Angew. Chem. 10.1002/ange.201912195

Link to VoR: <http://dx.doi.org/10.1002/anie.201912195>
<http://dx.doi.org/10.1002/ange.201912195>

COMMUNICATION

Solvent-Vapor-Induced Reversible Single-Crystal-to-Single-Crystal Transformation of a Triphosphaazatriangulene-based Metal–Organic Framework

Soichiro Nakatsuka,^[a] Yusuke Watanabe,^[a] Yoshinobu Kamakura,^[a] Satoshi Horike,^[b] Daisuke Tanaka,^[a] and Takuji Hatakeyama*^[a]

Abstract: A triphosphaazatriangulene (H_3L) was synthesized by way of an intramolecular triple phospho-Friedel–Crafts reaction. The H_3L triangulene contains three phosphinate groups and an extended π -conjugated framework, which enables the stimuli-responsive reversible transformation of $[Cu(HL)(DMSO)\cdot(MeOH)]_n$, a 3D-MOF that exhibits reversible sorption characteristics, into $(H_3L\cdot 0.5[Cu_2(OH)_4\cdot 6H_2O]\cdot 4H_2O)$, a 1D-columnar assembled proton-conducting material. The hydrophilic nature of the latter resulted in a proton conductivity of $5.5 \times 10^{-3} \text{ S}\cdot\text{cm}^{-1}$ at 95% relative humidity and 60 °C.

Among main-group-element-containing π -conjugated materials, π -conjugated organophosphorus materials are among the most attractive due to the pyramidal geometries and $\sigma^*-\pi^*$ interactions of their phosphorus atoms.^[1] Based on these attractive features, π -conjugated organophosphorus materials are used in a variety of applications, such as liquid crystals,^[2] organic electronics,^[3] electrochromic materials,^[4] and bioimaging probes,^[5] among others.^[6] Recently, the introduction of multiple phosphorus atoms into polycyclic aromatic hydrocarbons (PAHs) has been used to tune their three-dimensional (3D) structures and electronic properties,^[7] which realized the effective recognition of fullerenes^[7b] and cumulative anisotropies with large dipole moments.^[7d] On the other hand, compounds containing multiple phosphorus atoms have been used as efficient linkers in metal–organic frameworks (MOFs).^[8,9] In particular, phosphonate monoester groups ($-P(O)(OH)(OR)$) offer carboxylate-like coordination modes to form MOFs^[10] that are substantially chemically and thermally stable; these MOFs have been used as ion-exchange materials, proton conductors, catalysts, and sorbents.

Herein, we describe the design and synthesis of a novel triphosphaazatriangulene (H_3L , Figure 1a) that consists of a non-planar polycyclic aromatic skeleton with three peripheral phosphinate groups.^[11] Electrostatic-potential calculations clearly

show heterogeneous surface charge (Figure 1b). Negative electrostatic potential localized on the oxygen atoms of phosphinate groups, whereas the rest of H_3L has a slightly positive electrostatic potential. The larger variation around the oxygen atoms suggest that the hydrophobic π -conjugated moiety is surrounded by hydrophilic phosphinate groups. Based on these features, we envisaged a dual role for H_3L , namely as a scaffold for the construction of 3D-MOFs through phosphinate-metal linkages, and 1D-columnar assemblies through non-covalent π - π interactions (Figure 1c).

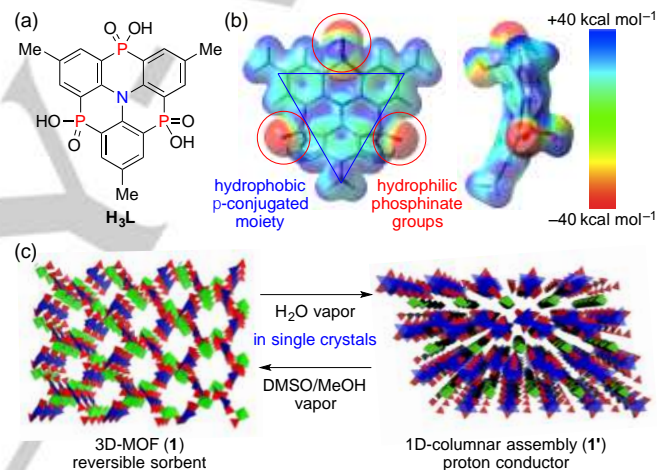


Figure 1. (a) Structure of triphosphaazatriangulene H_3L . (b) Molecular electrostatic potential surfaces of H_3L calculated at the B3LYP/6-31G(d) level of theory (color code: red = $-40 \text{ kcal mol}^{-1}$, blue = $+40 \text{ kcal mol}^{-1}$). (c) Illustrating the packing motif of the 3D-MOF and the 1D-columnar assembly.

After extensively screening metal salts and reaction conditions, we prepared $[Cu(HL)(DMSO)\cdot(MeOH)]_n$ (**1**), a copper-based 3D-MOF, that exhibits reversible MeOH-sorption behavior. Notably **1** is transformed into $H_3L\cdot 0.5[Cu_2(OH)_4\cdot 6H_2O]\cdot 4H_2O$ (**1'**), a 1D-columnar assembled material under high-humidity conditions, with the reverse process, the formation of MOF **1** from **1'**, occurring in a DMSO/MeOH-vapor atmosphere. These stimuli-responsive transformations were found to be reversible, even in a single crystal, due to the amphiphilic nature of H_3L and the moderate coordinating abilities of diaryl phosphinates. The 1D structure **1'** has hydrophilic domains composed of $Cu_2(OH)_4$ and H_2O , and exhibits a high proton conductivity of $5.5 \times 10^{-3} \text{ S}\cdot\text{cm}^{-1}$ at 95% relative humidity (RH) and 60 °C.

Triangulene H_3L was synthesized in five steps from tri-*p*-tolylamine (**2**) by the route shown in Figure 2. Tri-*p*-tolylamine **2** was first brominated with 3.1 equiv. of *N*-bromosuccinimide (NBS) to give the corresponding tribromide **3** in 94% yield. The initial

[a] Dr. Soichiro Nakatsuka, Yusuke Watanabe, Yoshinobu Kamakura, Prof. Daisuke Tanaka, Prof. Takuji Hatakeyama
Department of Chemistry
School of Science and Technology
Kwansei Gakuin University
2-1 Gakuen, Sanda
Hyogo 669-1337, Japan
E-mail: hatake@kwansei.ac.jp

[b] Prof. Satoshi Horike
Institute for Integrated Cell-Material Sciences
Institute for Advance Study
Kyoto University, Yoshida-Honmachi
Sakyo-ku, Kyoto, 606-8501 Japan

Supporting information for this article is given via a link at the end of the document.

COMMUNICATION

lithium–bromine exchange of **3** with 3.1 equiv. of butyllithium, subsequent trapping of the resulting aryllithium with 3.5 equiv. of bis(*N,N*-diethylamino)chlorophosphine, followed by sulfurization with 4.0 equiv. of S₈ afforded intermediate **4** in 65% yield. The triple intramolecular phospho-Friedel–Crafts reaction^[12] of **4** with 2.0 equiv. of *N,N*-diisopropylethylamine in the presence of 3.0 equiv. of AlCl₃ at 140 °C for 12 h afforded **5** in 47% yield. Oxidation with *m*-CPBA afforded the corresponding phosphine oxide **6** in 91% yield, with subsequent hydrolysis providing the desired H₃L ligand in 81% yield. A solution of H₃L in DMSO (1.0 × 10⁻² M) was mixed with CuSO₄·5H₂O in MeOH (1.0 × 10⁻² M) at 40 °C for 2 d to afford the [Cu(HL)(DMSO)·(MeOH)]_n MOF (**1**) in 46% yield as a yellow crystalline powder.

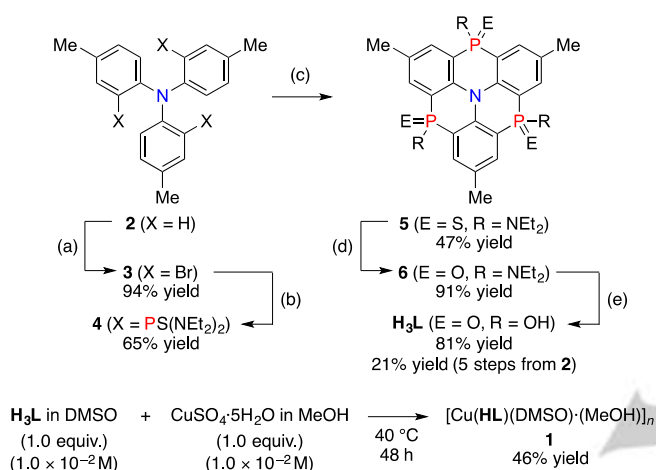


Figure 2. The six-step synthesis of **1**. Conditions: (a) *N*-bromosuccinimide (3.1 equiv.), CH₃CN, 0 °C, then room temperature, 19 h. (b) *n*-butyllithium (3.1 equiv.), toluene, 0 °C, then room temperature, 2 h; then bis(*N,N*-diethylamino)chlorophosphine (3.5 equiv.), toluene/ether (1:3 v/v), -78 °C, then 0 °C, 2 h; then S₈ (4.0 equiv.), toluene, 0 °C, then room temperature, 14 h. (c) AlCl₃ (3.0 equiv.), *N,N*-diisopropylethylamine (2.0 equiv.), *o*-dichlorobenzene, 0 °C, then room temperature, 12 h, then 140 °C, 12 h. (d) *m*-CPBA (12.0 equiv.), dichloromethane, -40 °C, 20 min. (e) 3 M aq. HCl/THF (1:1 v/v), 0 °C, then 60 °C, 8 h.

Single crystals suitable for X-ray crystallography were obtained by the slow-diffusion intermixing of a solution of CuSO₄·5H₂O in MeOH and H₃L in DMSO.^[13] Figure 3a shows the copper-coordination environment in **1**; the Cu²⁺ ions are trigonal-bipyramidally coordinated to the four O atoms of HL²⁻ and the oxygen atom of a DMSO. The Cu–O₂ and Cu–O₄ bond lengths are 1.904(2) and 1.925(3) Å, respectively, shorter than the Cu–O₁, Cu–O₃, and Cu–O₅ bond lengths (2.074(2), 1.986(2), and 2.080(3) Å, respectively). The framework of **1** is constructed from the Cu²⁺ center, which acts as a four-connected node using HL²⁻ as a four-connected linker (Figure 3b). This arrangement produces a large twelve-membered ring composed of six trigonal bipyramidal Cu²⁺ moieties linked together by six HL units. The framework expands in three directions to form a 3D network (Figure 3c). MOF **1** possesses straight 1D channels along the *a* axis that are occupied by MeOH molecules. In **1**, 10.9% of the total void volume per unit cell volume, V_{void}, is accessible to solvent molecules.^[14] DMSO molecules, which are highly ordered on the surfaces of the channels and coordinate to Cu²⁺, can

interact with guest molecules. The X-ray crystallographic data clearly reveal that MeOH molecules interact weakly through hydrogen bonds to the oxygen atoms of the DMSO molecules (O[MeOH]···O[DMSO] = ~2.9 Å).

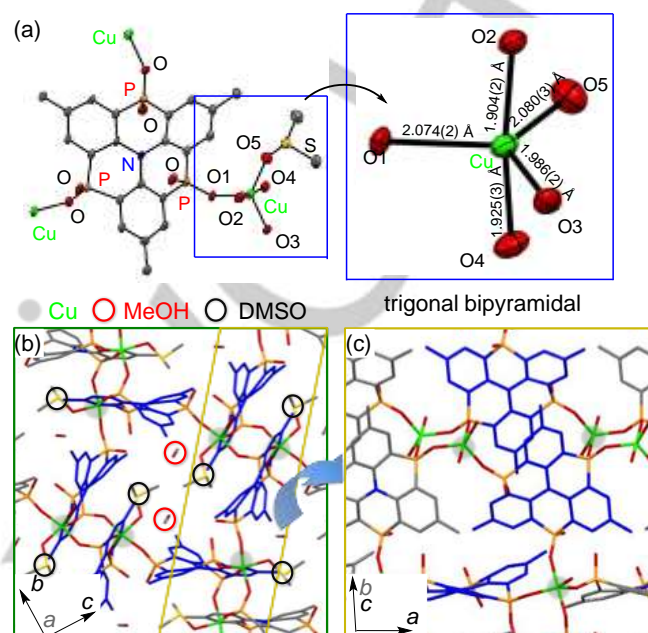


Figure 3. (a) The crystallographic environment around the Cu²⁺. (b, c) Two views of the packing structure of **1**. Hydrogen atoms and guests in the pores are omitted for clarity. Selected bond angles (°): O₁–Cu–O₅ = 120.48(11), O₁–Cu–O₃ = 111.59(10), O₃–Cu–O₅ = 127.93(11), O₂–Cu–O₄ = 170.20(12), O₁–Cu–O₂ = 91.81(10), O₂–Cu–O₅ = 85.64(11).

The methanol-sorption isotherms for **1** at 298 K shown in Figure 4b and the powder X-ray diffraction (PXRD) patterns shown in Figures S4 and S5 indicate that the framework is sufficiently flexible around the hydrophilic domain to absorb methanol vapor while maintaining its overall crystalline structure during the process. In order to examine its stimuli-responsive transformation, **1** was exposed to water vapor in air for 1 week, during which time the color of the crystal was observed to slowly change from the yellow of **1** to the blue-green of **1'**, the 1D-columnar assembled material. This transformation was complete within 12 h when the MeOH in **1** was removed *in vacuo*. Surprisingly, these crystals were persistently single-crystalline following this transformation. The single-crystal X-ray structure of **1'** shows that the cell volume of the material had increased from 2583.84(9) to 2819.2 (1409.6(15) × 2) Å³. Full assignment of the structure of **1'** shows that the DMSO in **1** has been removed and that **1** has been completely converted into H₃L·0.5[Cu₂(OH)₄·6H₂O]·4H₂O, a 1D-columnar assembled material of H₃L and Cu₂(OH)₄ in single crystals (Figure 4a). A comparison of the structural features of **1** and **1'** helps to reveal the mechanism of the single-crystal-to-single-crystal (SC-SC) transformation. We hypothesize that H₂O molecules coordinate to the Cu²⁺ center and the phosphonate groups, with the DMSO in **1** cleaved from the Cu²⁺ center. Three aquo and two hydroxo ligands replace the cleaved coordinating phosphonate groups and DMSO to maintain a trigonal bipyramidal geometry. In addition, the resulting hydrophilic domain of Cu(OH)₂·3H₂O is

COMMUNICATION

pushed outward to form straight 1D channels due to the hydrophobic π -conjugated H_3L moiety; the overall result of this process is the formation of edge-sharing octahedral dimers. H_3L is densely accumulated in $\mathbf{1}'$ through intermolecular non-covalent contacts, and the 1D-columnar assembly of H_3L is stabilized by the hydrophilic 1D $\text{Cu}_2(\text{OH})_4$ and H_2O domains through intermolecular hydrogen bonding. Moreover, $\mathbf{1}$ was reconstructed within the single crystal upon exposure of $\mathbf{1}'$ to DMSO/MeOH vapor. Thus, 3D-MOF and 1D-columnar assembled materials are formed reversibly in response to changes in solvent vapor through the dual role played by H_3L .

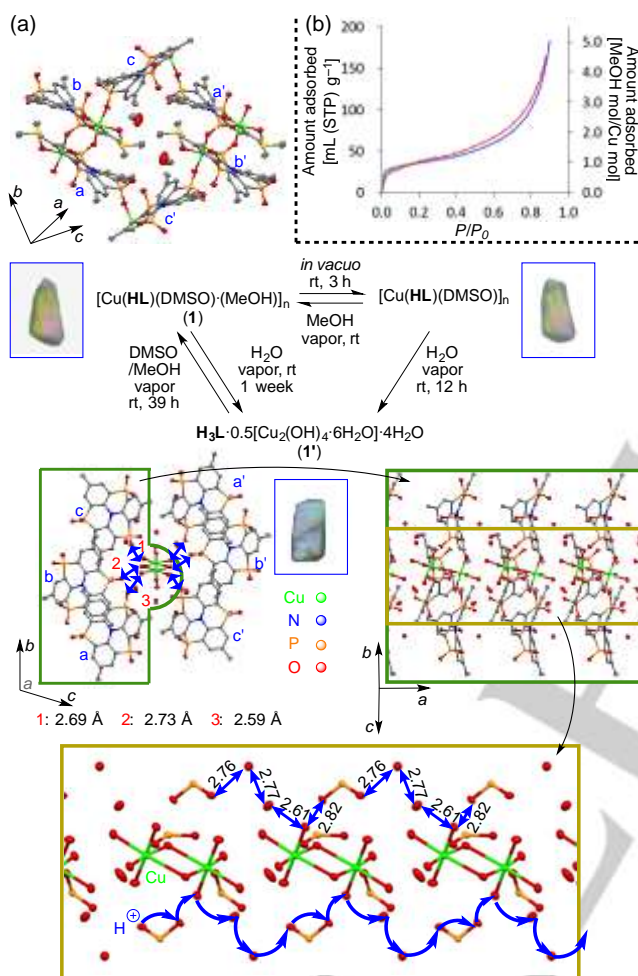


Figure 4. (a) Reversible formation of (top-left) $\mathbf{1}$ showing a MeOH-filled channel and (middle) $\mathbf{1}'$ showing H₂O-filled channels in a single crystal. Enlarged view of the packing structure of $\mathbf{1}'$ (bottom). The blue arrows show H₃L-to-H₂O, H₃L-to-Cu₂(OH)₄·6H₂O, and H₂O-to-Cu₂(OH)₄·6H₂O interactions that create an extended H-bonding network along the 1D channels to build a potential proton-transfer pathway. Thermal ellipsoids are shown at the 50% probability level and H atoms are omitted for clarity. (b) Methanol-sorption isotherms at 25 °C for $\mathbf{1}$.

The presence of an extended hydrogen-bonded network and the additional protons from the phosphinic acid ($-\text{P}(\text{O})(\text{OH})$) in H_3L , $\text{Cu}_2(\text{OH})_4$, and the water molecules that form 1D channels reveal that $\mathbf{1}'$ is potentially a highly proton-conducting material.

To characterize its proton conductivity, $\mathbf{1}$ was subjected to AC impedance spectroscopy under conditions of controlled humidity (Figures S10) and temperature after the MeOH in $\mathbf{1}$ had been removed *in vacuo* (Figure S13). Prior to any impedance experiment, the phase purity of the bulk sample was confirmed by powder X-ray diffractometry (PXRD, Figure S5). The proton conductivity was found to be $5.9 \times 10^{-8} \text{ S cm}^{-1}$ at 25 °C and 55% relative humidity (RH). Nyquist plots under a variety of humidity conditions (from 55% to 95% RH) at 25 °C show that conductivity increases with increasing RH (Figure S10 and S13a) because the water molecules adsorbed in the voids of $\mathbf{1}$ assist with proton diffusion. The Nyquist plot shown in Figure S13a reveals that a higher proton conductivity of $7.4 \times 10^{-4} \text{ S cm}^{-1}$ is observed at 25 °C and 95% RH. The color of the pellet and the PXRD pattern acquired at 95% RH (Figure S5) suggests the formation of $\mathbf{1}'$, which has proton-transport pathways with stabilized hydrophilic domains. The conductivity was $5.5 \times 10^{-3} \text{ S cm}^{-1}$ at 60 °C and 95% RH. The Arrhenius plot provided a linear fit, from which the activation energy for proton conduction was determined to be 0.52 eV on the basis of impedance spectra recorded between 25 and 60 °C at 95% RH (Figure S14). We found that H_3L plays an important role in creating proton-conducting pathways; that is, the hydrophilic domain is stabilized by the peripheral hydrophilic phosphinate groups of the H_3L hydrophobic core.

In summary, we successfully synthesized H_3L , a new triphosphaazatriangulene, through the use of a triple phospho-Friedel-Crafts reaction. H_3L has a hydrophobic extended π -conjugated framework surrounded by hydrophilic phosphinate groups, which is an attractive feature. Based on the amphiphilic nature of H_3L , external stimuli trigger transformations between the 3D-MOF $\mathbf{1}$ with reversible MeOH-sorption characteristics and the 1D-columnar assembled material $\mathbf{1}'$ with high proton conductivity. Even though this transformation involves the cooperative breakage/formation of metal-phosphinate coordination bonds, these transformations are single-crystal-to-single-crystal (SC-SC) processes due to the dual assembly state nature of H_3L , which will contribute to the design and synthesis of new smart materials.

Acknowledgements

This study was supported by a Grant-in-Aid for Scientific Research (JP18H02051) and Challenging Research (Exploratory, JP19K22191) from JSPS, and CREST (JPMJCR18R3) programs from JST. Preliminary measurements for the X-ray crystal structure analysis were performed at the BL40XU beamline in SPring-8 with the approval of JASRI (2017A1132, 2017B1073, 2018A1114, 2018B1125, 2019A1142) and with the help of Dr. Nobuhiro Yasuda (JASRI). We thank Prof. Hirofumi Yoshikawa (Kwansei Gakuin University) for allowing us to use gas adsorption analyzer and Ms. Nanae Shimanaka (Kyoto University) for supporting conductivity measurement.

Keywords: Metal-organic frameworks • Phosphorus • Polycycles • Phospha-Friedel-Crafts reaction • Proton transport

COMMUNICATION

- [1] Recent reviews: a) E. Regulska, C. Romero-Nieto, *Dalton. Trans.* **2018**, 47, 10344–10359; b) R. Szűcs, P.-A. Bouit, L. Nyulási, M. Hissler, *ChemPhysChem* **2017**, 18, 2618–2630; c) D. Joly, P.-A. Bouit, M. Hissler, *J. Mater. Chem. C* **2016**, 4, 3686–3698. d) T. Baumgartner, *Acc. Chem. Res.* **2014**, 47, 1613–1622; e) M. Stolar, T. Baumgartner, *Chem. - An Asian J.* **2014**, 9, 1212–1225.
- [2] a) Z. Wang, B. S. Gelfand, P. Dong, S. Trudel, T. Baumgartner, *J. Mater. Chem. C* **2016**, 4, 2936–2944; b) Z. Wang, B. S. Gelfand, T. Baumgartner, *Angew. Chem. Int. Ed.* **2016**, 55, 3481–3485; *Angew. Chem.* **2016**, 128, 3542–3546; c) Y. Ren, W. H. Kan, M. A. Henderson, P. G. Bomben, C. P. Berlinguette, V. Thangadurai, T. Baumgartner, *J. Am. Chem. Soc.* **2011**, 133, 17014–17026; d) C. Romero-Nieto, M. Marcos, S. Merino, J. Barberá, T. Baumgartner, J. Rodríguez-López, *Adv. Funct. Mater.* **2011**, 21, 4088–4099.
- [3] For OLEDs: a) P. Hindenberg, J. Zimmermann, G. Hernandez-Sosa, C. Romero-Nieto, *Dalton. Trans.* **2019**, 48, 7503–7508; b) H. Gotoh, S. Nakatsuka, Y. Kondo, Y. Sasada, T. Hatakeyama, *Chem. Lett.* **2018**, 47, 920–922; c) S. Nakatsuka, H. Gotoh, A. Kageyama, Y. Sasada, T. Ikuta, T. Hatakeyama, *Organometallics* **2017**, 36, 2622–2631; d) F. Riobé, R. Szűcs, P. A. Bouit, D. Tondelier, B. Geffroy, F. Aparicio, J. Buendía, L. Sánchez, R. Réau, L. Nyulási, et al., *Chem. - A Eur. J.* **2015**, 21, 6547–6556; e) H. C. Su, O. Fadel, C. J. Yang, T. Y. Cho, C. Fave, M. Hissler, C. C. Wu, R. Réau, *J. Am. Chem. Soc.* **2006**, 128, 983–995; For OPVs: f) Y. Matano, H. Ohkubo, T. Miyata, Y. Watanabe, Y. Hayashi, T. Umeyama, H. Imahori, *Eur. J. Inorg. Chem.* **2014**, 2014, 1620–1624; g) Y. Matano, A. Saito, Y. Suzuki, T. Miyajima, S. Akiyama, S. Otsubo, E. Nakamoto, S. Aramaki, H. Imahori, *Chem. - An Asian J.* **2012**, 7, 2305–2312; h) H. Tsuji, K. Sato, Y. Sato, E. Nakamura, *Chem. - An Asian J.* **2010**, 5, 1294–1297.
- [4] a) Z. Lian, B. N. Bhawal, P. Yu, B. Morandi, *Science* **2017**, 356, 1059–1063; b) N. Yoshikai, M. Santra, B. Wu, *Organometallics* **2017**, 36, 2637–2645; c) C. Reus, T. Baumgartner, *Dalton. Trans.* **2016**, 45, 1850–1855; d) E. Yamaguchi, C. Wang, A. Fukazawa, M. Taki, Y. Sato, T. Sasaki, M. Ueda, N. Sasaki, T. Higashiyama, S. Yamaguchi, *Angew. Chem. Int. Ed.* **2015**, 54, 4539–4543; *Angew. Chem.* **2015**, 127, 4622–4626; e) M. Stolar, J. Borau-Garcia, M. Toonen, T. Baumgartner, *J. Am. Chem. Soc.* **2015**, 137, 3366–3371.
- [5] a) C. Wang, M. Taki, Y. Sato, A. Fukazawa, T. Higashiyama, S. Yamaguchi, *J. Am. Chem. Soc.* **2017**, 139, 10374–10381; b) A. Fukazawa, S. Suda, M. Taki, E. Yamaguchi, M. Grzybowski, Y. Sato, T. Higashiyama, S. Yamaguchi, *Chem. Commun.* **2016**, 52, 1120–1123; c) X. Chai, X. Cui, B. Wang, F. Yang, Y. Cai, Q. Wu, T. Wang, *Chem. - A Eur. J.* **2015**, 21, 16754–16758; d) M. Taki, H. Ogasawara, H. Osaki, A. Fukazawa, Y. Sato, K. Ogasawara, T. Higashiyama, S. Yamaguchi, *Chem. Commun.* **2015**, 51, 11880–11883; e) X. D. Jiang, J. Zhao, D. Xi, H. Yu, J. Guan, S. Li, C. L. Sun, L. J. Xiao, *Chem. - A Eur. J.* **2015**, 21, 6079–6082.
- [6] a) C. Wang, A. Fukazawa, Y. Tanabe, N. Inai, D. Yokogawa, S. Yamaguchi, *Chem. - An Asian J.* **2018**, 13, 1616–1624; b) Z. Zhang, Z. Wang, M. Haehnel, A. Eichhorn, R. M. Edkins, A. Steffen, A. Krueger, Z. Lin, T. B. Marder, *Chem. Commun.* **2016**, 52, 9707–9710; c) M. Yamamura, T. Saito, T. Nabeshima, *J. Am. Chem. Soc.* **2014**, 136, 14299–14306; d) X. He, P. Zhang, J.-B. Lin, H. V. Huynh, S. E. Navarro Muñoz, C.-C. Ling, T. Baumgartner, *Org. Lett.* **2013**, 15, 5322–5325; e) A. Kira, Y. Shibano, S. Kang, H. Hayashi, T. Umeyama, Y. Matano, H. Imahori, *Chem. Lett.* **2010**, 39, 448–450.
- [7] a) S. Furukawa, Y. Suda, J. Kobayashi, T. Kawashima, T. Tada, S. Fujii, M. Kiguchi, M. Saito, *J. Am. Chem. Soc.* **2017**, 139, 5787–5792; b) T. W. Greulich, E. Yamaguchi, C. Doerenkamp, M. Lübbesmeier, C. G. Daniliuc, A. Fukazawa, H. Eckert, S. Yamaguchi, A. Studer, *Chem. - A Eur. J.* **2017**, 23, 6029–6033; c) M. Yamamura, D. Hongo, T. Nabeshima, *Chem. Sci.* **2015**, 6, 6373–6378; d) S. Hashimoto, S. Nakatsuka, M. Nakamura, T. Hatakeyama, *Angew. Chem. Int. Ed.* **2014**, 53, 14074–14076; *Angew. Chem.* **2014**, 126, 14298–14300.
- [8] a) A. Schneemann, V. Bon, I. Schwedler, I. Senkovska, S. Kaskel, R. A. Fischer, *Chem. Soc. Rev.* **2014**, 43, 6062; b) T. Devic, C. Serre, *Chem. Soc. Rev.* **2014**, 43, 6097; c) H. Furukawa, K. E. Cordova, M. O'Keeffe, O. M. Yaghi, *Science* **2013**, 341, 974; d) L. E. Kreno, K. Leong, O. K. Farha, M. Allendorf, R. P. Van Duyne, J. T. Hupp, *Chem. Rev.* **2012**, 112, 1105; e) G. Ferey, *Chem. Soc. Rev.*, **2008**, 37, 191.
- [9] a) I. Carson, M. R. Healy, E. D. Doidge, J. B. Love, C. A. Morrison, P. A. Tasker, *Coord. Chem. Rev.* **2017**, 335, 150–171; b) J. Goura, V. Chandrasekhar, *Chem. Rev.* **2015**, 115, 6854–6965; c) K. J. Gagnon, H. P. Perry, A. Clearfield, *Chem. Rev.* **2012**, 112, 1034–1054; d) G. K. H. Shimizu, R. Vaidhyanathan, J. M. Taylor, *Chem. Soc. Rev.* **2009**, 38, 1430–1449.
- [10] a) J. Hynek, P. Brázda, J. Rohlíček, M. G. S. Londesborough, J. Demel, *Angew. Chem. Int. Ed.* **2018**, 57, 5016–5019; *Angew. Chem.* **2018**, 130, 5110–5113; b) B. Joarder, J. Bin Lin, Z. Romero, G. K. H. Shimizu, *J. Am. Chem. Soc.* **2017**, 139, 7176–7179; c) N. E. Wong, P. Ramaswamy, A. S. Lee, B. S. Gelfand, K. J. Bladec, J. M. Taylor, D. M. Spasyuk, G. K. H. Shimizu, *J. Am. Chem. Soc.* **2017**, 139, 14676–14683; d) B. S. Gelfand, R. P. S. Huynh, R. K. Mah, G. K. H. Shimizu, *Angew. Chem. Int. Ed.* **2016**, 55, 14614–14617; *Angew. Chem.* **2016**, 128, 14834–14837; e) J. M. Taylor, R. Vaidhyanathan, S. S. Iremonger, G. K. H. Shimizu, *J. Am. Chem. Soc.* **2012**, 134, 14338–14340; f) S. S. Iremonger, J. Liang, R. Vaidhyanathan, I. Martens, G. K. H. Shimizu, T. D. Daff, M. Z. Aghaji, S. Yeganegi, T. K. Woo, *J. Am. Chem. Soc.* **2011**, 133, 20048–20051.
- [11] a) A. Winter, U. S. Schubert, *Mater. Chem. Front.* **2019**, 3, 2308–2325; b) M. Hirai, N. Tanaka, M. Sakai, S. Yamaguchi, *Chem. Rev.* **2019**, 119, 8291–8331; c) N. Hammer, T. A. Schaub, U. Meinhardt, M. Kivala, *Chem. Rec.* **2015**, 15, 1119–1131.
- [12] a) S. Nakatsuka, H. Gotoh, K. Kinoshita, N. Yasuda, T. Hatakeyama, *Angew. Chem. Int. Ed.* **2017**, 56, 5087–5090; *Angew. Chem.* **2017**, 129, 5169–5172; b) Y. Unoh, Y. Yokoyama, T. Satoh, K. Hirano, M. Miura, *Org. Lett.* **2016**, 18, 5436–5439; c) Y. Unoh, T. Satoh, K. Hirano, M. Miura, *ACS Catal.* **2015**, 5, 6634–6639; d) C. Romero-Nieto, A. López-Andarias, C. Egler-Lucas, F. Gebert, J. P. Neus, O. Pilgram, *Angew. Chem. Int. Ed.* **2015**, 54, 15872–15875; *Angew. Chem.* **2015**, 127, 16098–16102; e) T. Hatakeyama, S. Hashimoto, M. Nakamura, *Org. Lett.* **2011**, 13, 2130–2133.
- [13] S. Masaoka, D. Tanaka, H. Kitahata, S. Araki, R. Matsuda, K. Yoshikawa, K. Kato, M. Takata, S. Kitagawa, *J. Am. Chem. Soc.* **2006**, 128, 15799–15808.
- [14] Spek, A. L. PLATON, A Multipurpose Crystallographic Tool; Utrecht University: Utrecht, The Netherlands, 2001.

WILEY-VCH

Accepted Manuscript